

# Laser and transistor material on Si substrate

Dzianis Saladukha<sup>a,b</sup>, Tomasz J. Ochalski<sup>a,b</sup>, Felipe Murphy Armando<sup>a</sup>, Michael B. Clavel<sup>c</sup>,  
Mantu K Hudait<sup>c</sup>

<sup>a</sup>Tyndall National Institute, Lee Maltings, Dyke Parade, Cork, Ireland;

<sup>b</sup>Cork Institute of Technology, Rossa Ave, Co. Cork, Ireland

<sup>c</sup>Advanced Devices & Sustainable Energy Laboratory (ADSEL), Bradley Department of Electrical and Computer Engineering, Virginia Tech, Blacksburg, Virginia 24061, USA

## ABSTRACT

In this work we study Ge structures grown on silicon substrates. We use photoluminescence and photoreflectance to determine both direct and indirect gap of Ge under tensile strain. The strain is induced by growing the Ge on an InGaAs buffer layer with variable In content. The band energy levels are modeled by a 30 band k-p model based on first principles calculations. Characterization techniques show very good agreement with the calculated energy values.

**Keywords:** Ge photoluminescence, photoreflectance, tensile Ge, Ge Si, Ge on InGaAs, Ge TFeT, Ge biaxial strain

## 1. INTRODUCTION

Further increases in transistor clock speeds are limited by heat dissipation on chip [1], [2]. One way to reduce this dissipation is, for example, by selecting transistor channel materials with low threshold voltage and high charge carrier mobility. A potential candidate to replace Si as a suitable channel material is Ge [3], [4]. Tensile strained Ge has a significantly higher n-type mobility [5], which has a profound impact on the transistor switch rate.

Optical integration of laser-on-chip has wide range of applications and requires laser manufacturing compatible with Si-based technology. However there are number of challenges. Firstly, Si itself is not a direct band gap material and is therefore an inefficient light emitter. The absence of lasers on Si is a significant problem for optical integration in CMOS. Secondly, most conventional III-V materials typically have a large lattice mismatch and different thermal expansion coefficients from Si [6]. In the case of direct growth of such III-V materials on silicon, they suffer from a high-density of threading dislocations and thus have a limited suitability for laser applications, though there are a few reports on GaAs-based lasers grown on a Si substrate [7]. An alternative method would be using Ge as a laser material. There are number of approaches for designing of Ge energy diagram [8-11]. Under tensile strain, the bottom of the Ge  $\Gamma$ -valley decreases in energy faster than the L-valley, thereby potentially making Ge a direct bandgap semiconductor. However when grown directly on silicon, Ge is compressively strained. In order to achieve tensile strain one needs to grow a buffer with a larger lattice parameter than that of Ge. GaAs is nearly lattice matched to Ge (-0.12% of mismatch). By adding In in to the GaAs buffer, one can increase the lattice constant of the InGaAs layer and thus induce a biaxial tensile strain to the Ge. In this work, the energy positions of the  $\Gamma$  and L valleys of Ge grown on InGaAs buffers with different In content are studied by means of photoluminescence spectroscopy.

## 2. THEORETICAL CALCULATIONS

The Ge band alignment grown on InGaAs depends on the InGaAs layer surface termination (figure 1). If the InGaAs surface is terminated on the As atomic layer, the Ge valence band has a lower band edge than that of InGaAs. The valence band offset is 0.12 eV for Ge on In<sub>0.13</sub>Ga<sub>0.87</sub>As and 0.10 eV for In<sub>0.17</sub>Ga<sub>0.83</sub>As. In this case, band alignment between Ge and InGaAs is type II. However if the InGaAs surface is terminated on the Ga or In atomic layer, the Ge valence band is higher than that of the InGaAs layer, leading to a type I band alignment. We calculate the Ge band structure within a 30 band k.p formalism, based on GW calculations [12], [13]. The different energy transitions as a function of strain in the Ge layer are presented in figure 2. The blue and red lines correspond to the L and  $\Gamma$  band minima, respectively. Under tensile strain, the degeneracy of the light-holes and heavy-holes at the zone center split. The solid and dashed lines correspond to light-hole (lh) and heavy-hole (hh) transitions respectively. To avoid strain relaxation in the material, the Ge layers are grown below the critical thickness: 40nm and 30nm for the lower and higher strain structures, respectively. Quantum confined energy levels in these thin layers are shown in figure 2 as dot and dash-dot lines. The experimentally measured

values of  $\Gamma$ -hh and L-lh energy transitions are also presented in the figure for approximate values of 0% and 1.1% tensile strain. According to the band energy calculations Ge should switch band gap type from indirect to direct under a 1.5% biaxial tensile strain.

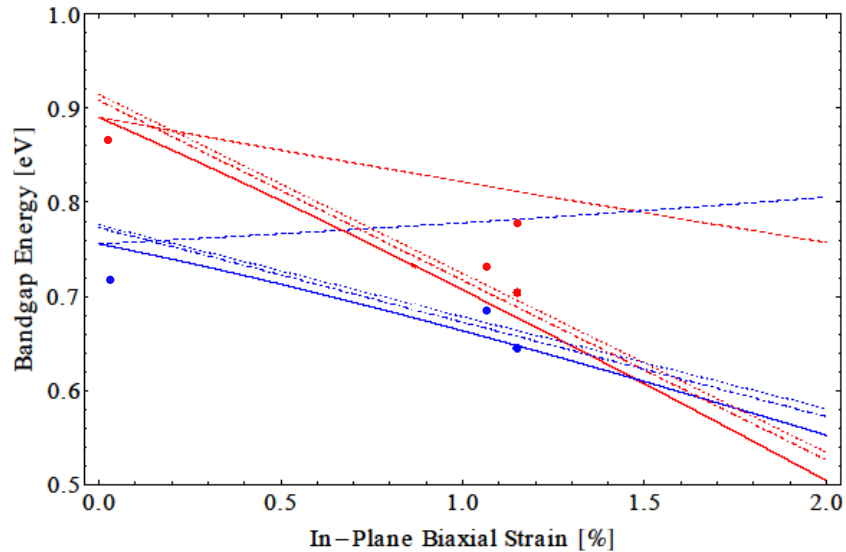


Figure 1. Ge L and  $\Gamma$  band energy calculations. Band minimum is depicted: L-lh – blue solid line,  $\Gamma$ -lh – red solid line, L-hh – blue dashed line,  $\Gamma$ -hh – red dashed line; electron energy levels for 30nm quantum well - dash-dot and dot lines; experimental peak points – red and blue dots.

### 3. SAMPLES DESCRIPTION

We performed an optical study of the multilayer transistor structures, presented in figure 3. Samples *a*, *b* are grown on a Si substrate, followed by a GaAs layer and sample *c* was grown directly on GaAs substrate. Samples *b*, *c* have  $\text{In}_x\text{Ga}_{1-x}\text{As}$  linear-graded barrier with a slow increase of In-content. Samples presented in this paper have a gradient from 0 up to 16% and 17% In content. On the top of  $\text{In}_{0.16}\text{Ga}_{0.84}\text{As}$  and  $\text{In}_{0.17}\text{Ga}_{0.83}\text{As}$  layers there is a 15nm and 30nm layer of Ge, respectively. Unstrained Ge was studied at pure Ge wafer. Lattice mismatch between  $\text{In}_{0.16}\text{Ga}_{0.84}\text{As}$  and Ge is 1.05% (sample *c*) while between  $\text{In}_{0.17}\text{Ga}_{0.83}\text{As}$  and Ge it is 1.11% (samples *b*) hence defining the corresponding level of tensile strain in Ge. Both samples have very close strain. In order to provide better charge carrier trapping to Ge layer at photoluminescence, sample *c* has an GaAs cap layer on the top of Ge. Complete growth details are described in the previous work [14].

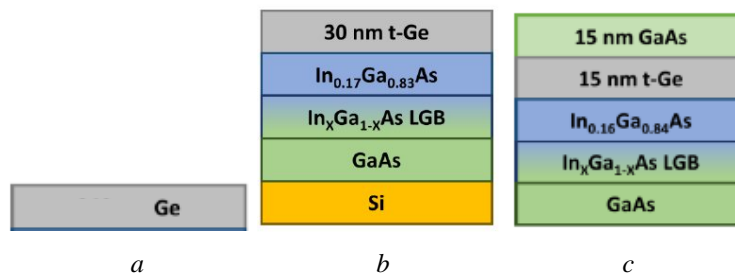


Figure 2. Samples material structure with a – 0%, b – 1.11%, c – 1.05% tensile strain applied to Ge

### 4. EXPERIMENTAL SETUP

For material description, we performed a conventional photoluminescence spectroscopy measurement and photoreflectance [15] characterization. Photoreflectance experimental setup is presented in Figure 5. Technique is based on sample's refractive index change under influence of high electric field. 405nm diode laser stimulated photoexcitation of electric field at the surface of the samples. Samples were put in a liquid nitrogen cryostat and chilled to 77K. Reflection

spectra was measured by liquid nitrogen chilled InAs detector and using monochromator with broad light source at one slit as a tunable light source.

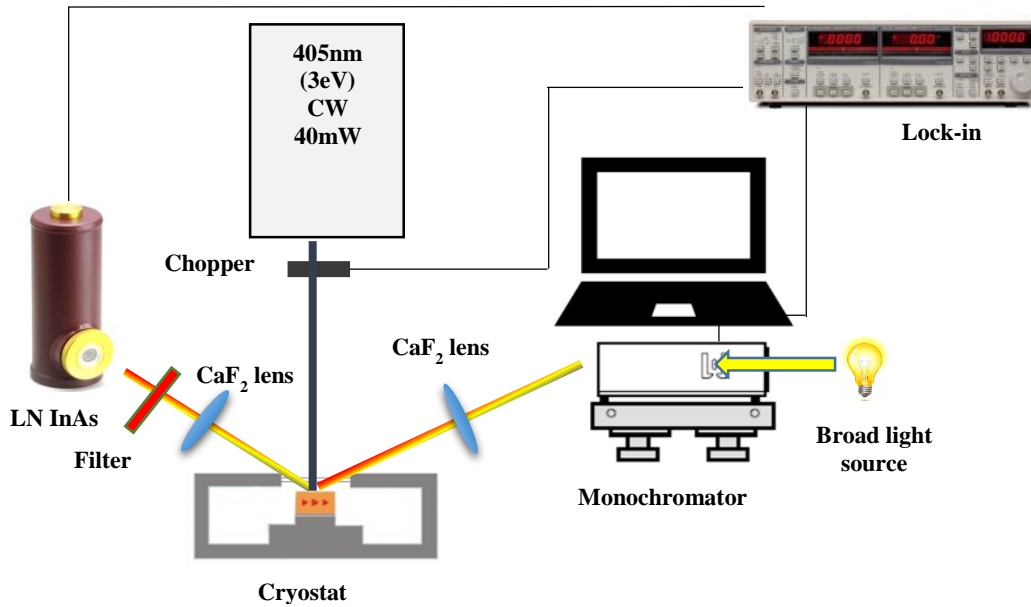


Figure 3. Photoreflectance spectroscopy setup

## 5. RESULT DISCUSSION

The measured photoluminescence spectrum of sample *a* is presented in figure 5. It is fitted with a Gaussian peak, representing the L-lh energy transition. Theoretical value of bulk Ge L-lh transition is 0.76 eV. From the experiment, the  $\Gamma$ -lh transition is at 0.714 eV.

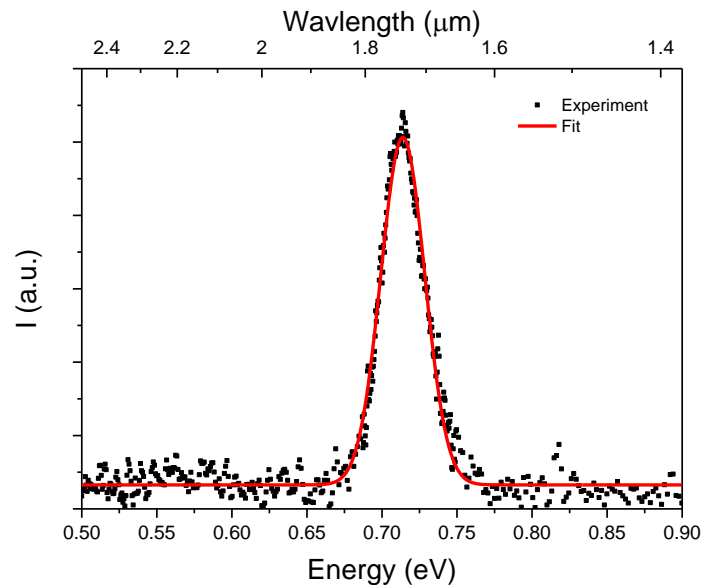


Figure 4. Sample *a* photoluminescence spectra. Black dots corresponds to experimental data, red line – Gaussian fit

For sample *b*, under  $\epsilon=1.11\%$  tensile strain, the photoluminescence spectrum is presented in figure 6. There is a clear shift of photoluminescence to lower energies for this sample in comparison to *a* sample without a strain. A Gaussian approximation with 3 peaks at 0.72 eV, 0.64 eV and 0.62 eV is fit to the experimental data, corresponding to the  $\Gamma$ -lh, L-lh and Type II transition energies. Calculated band edges of Ge under  $\epsilon=1.11\%$  tensile strain are 0.65eV for L-lh transition and 0.68 eV for  $\Gamma$ -lh transition. There is a 0.04eV difference for  $\Gamma$ -lh transitions between the fitted and calculated values. We speculate that this is due to strain relaxation of the Ge layer as well as broad nature of photoluminescence around  $\Gamma$ -lh transition peak. The valence band offset is calculated to be 0.10eV. The small peak around 0.60 eV represents a Type II transition from the Ge  $\Gamma$ -valley conduction band to the InGaAs valence band.

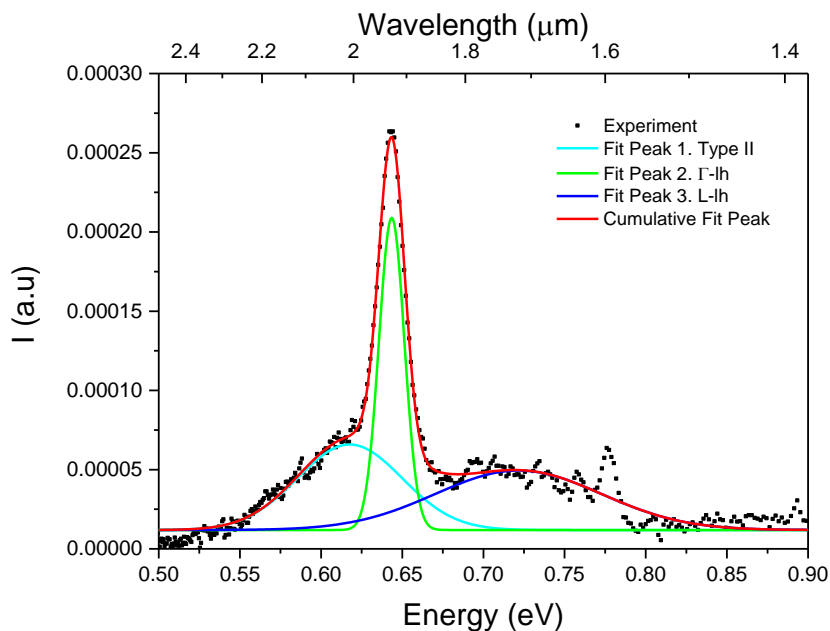


Figure 5. Sample *b* photoluminescence spectra. Black dots corresponds to experimental data, red line – Gaussian fit with 2 replicas. Cyan line corresponds to Type II transition from Ge conduction band to InGaAs valence band; Green line corresponds to L-lh transition; Blue line corresponds to  $\Gamma$ -lh transition

In order to improve carriers capture to Ge layer a thin GaAs layer was deposited on the top of Ge. Emission from sample *c* is presented in Figures 7. The peaks positions of the spectra are shifter to 0.684 eV for L-lh transition and 0.73eV for  $\Gamma$ -lh. According to model this values are 0.2eV higher then calculated values on Figure 1. This is related to higher quantum confinement of Ge in the sample *c* in comparison to samples *a* and *b*.

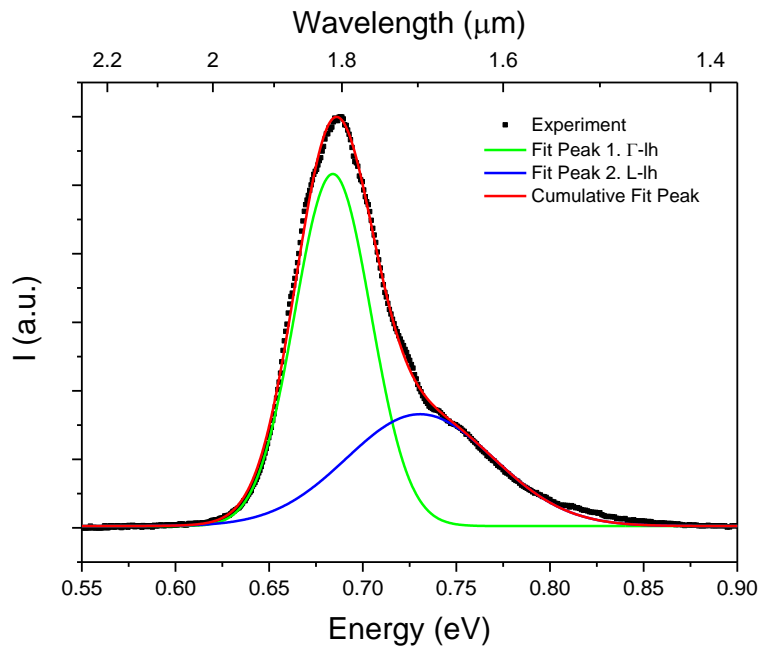


Figure 6. Sample *c* photoluminescence spectra. Black dots corresponds to experimental data, red line – Gaussian fit with 1 replica. Green line corresponds to L-Ih transition; Blue line corresponds to  $\Gamma$ -Ih transition

Deposition of cap GaAs layer on Ge provided an efficient barrier for charge carriers. This made possible detection of indirect PL up to room temperature. In Figure 8 one can see photoluminescence of sample *c* depending on temperature. Line on the plot corresponds to Gaussian peak position.

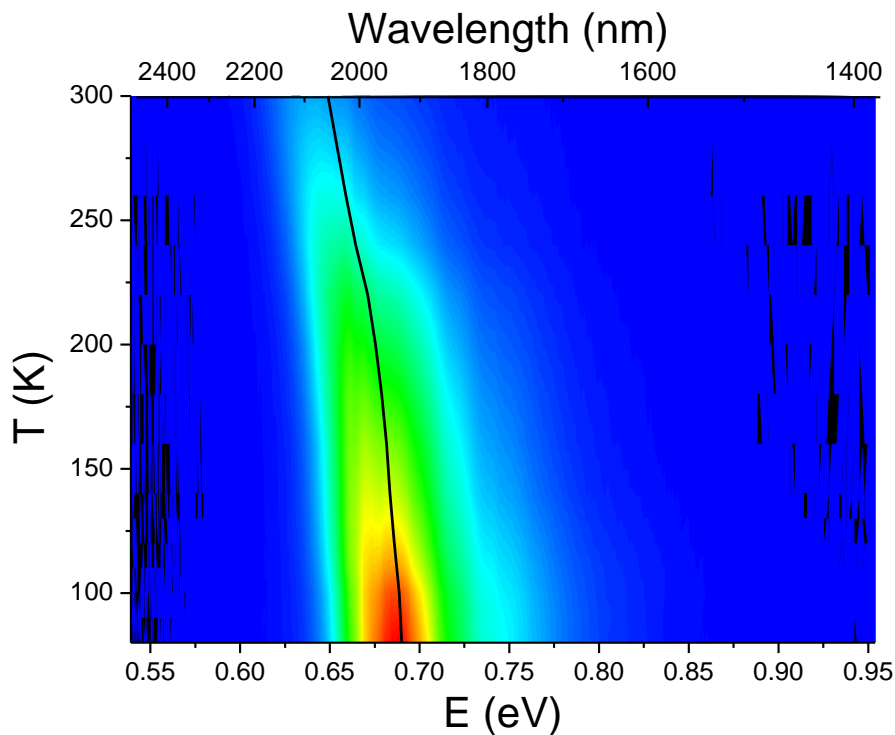


Figure 7. Sample *c* photoluminescence temperature map spectra. Red corresponds to high intensity, blue –to low; black line corresponds to Gaussian peak position

Photoreflection (PR) measurements of the samples *a, b* are shown in Figures 9, 10. Measurements were fitted with complex electro optical Airy function [16]. Critical energy in this fit corresponds energy level of semiconductor. For sample *a* a critical point found at 0.86 eV, what is quite close to theoretical value of 0.89 eV of  $\Gamma$  valley of unstrained Ge. Sample *b* with higher strain has critical point at 0.78 eV, which is relevant to 0.81 eV theoretical calculated value for  $\Gamma$ -hh transition. Sample *c* is not suitable for PR measurements, because it has a cap layer on the top. Electric field generated by exiting laser is dying fast in the plane of sample, so GaAs cap layer, provided efficient PL from *c* sample preserved it from PR one.

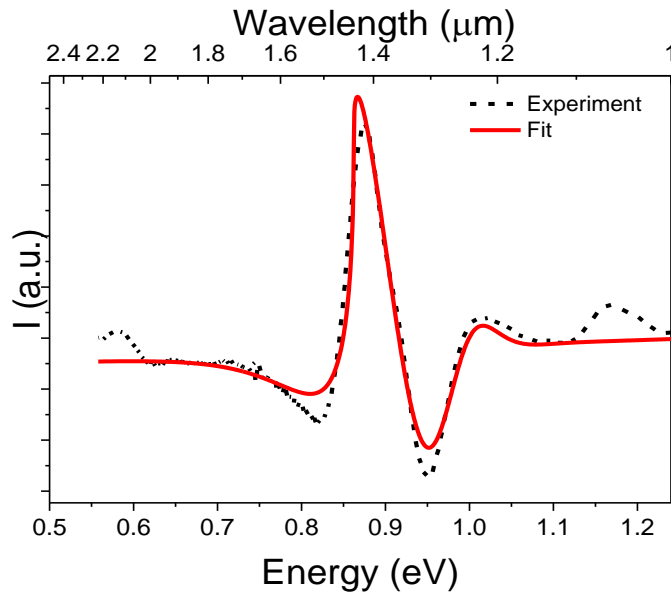


Figure 8. Sample *a* photoreflectance spectrum. Black dashed line corresponds to experimental data, red straight line – complex Airy approximation.

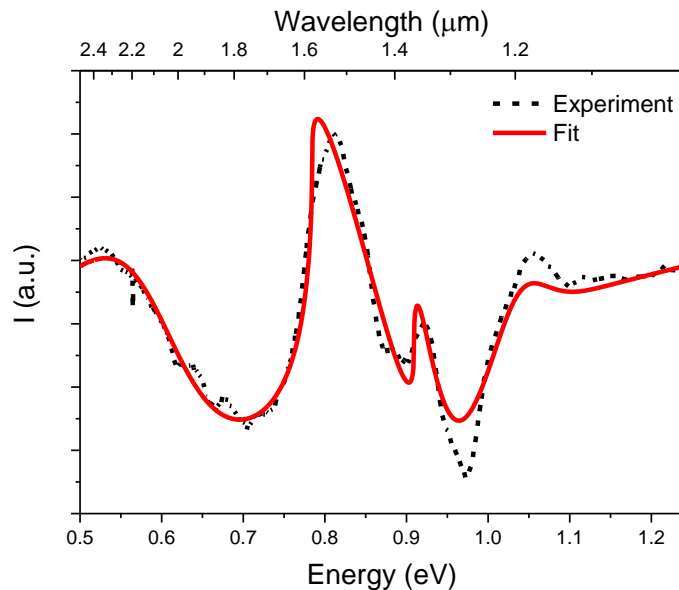


Figure 9. Sample *b* photoreflectance spectrum. Black dashed line corresponds to experimental data, red straight line – complex Airy approximation with one replica.

## 6. CONCLUSIONS

In this paper we presented photoluminescence and photoreflectance study of Ge TFET structures and presented a way to position both minimum and direct energy transitions of the material. Tensile strain was applied to Ge by growth on an InGaAs buffer layer with variable In content. We observed red-shift of both  $\Gamma$  and L bands with increase in tensile strain in the Ge layer from bulk material to 1.11% of strain. We were able to localize  $\Gamma$ -lh and L-lh energy transitions as well as presence of  $\Gamma$ -hh and Type II transitions from Ge to InGaAs.

## ACKNOWLEDGMENTS

The research in this publication was supported in part by a grant from Science Foundation Ireland (SFI) under the US-Ireland R&D Partnership Programme Grant No. SFI/14/US/I3057. This research was also supported in part by the National Science Foundation (US) under grant number ECCS-1348653 and through the NSF-sponsored joint US-Ireland R&D Partnership, grant number ECCS-1507950.

## REFERENCES

- [1] Clavel, M., Goley, P., Jain, N., Zhu, Y., Hudait, M.K. "Strain-Engineered Biaxial Tensile Epitaxial Germanium for High-Performance Ge/InGaAs Tunnel Field-Effect Transistors," *IEEE J. Electron Dev. Soc* 3(3), 184- 193 (2015).
- [2] Borkar, S., Karnik, T., Narendra, S., Tschanz, J., Keshavarzi, A., Vivek De., "Parameter Variations and Impact on Circuits and Microarchitecture," *Proc. Design Automation Conference* 40, 338-342 (2003).
- [3] Krishnamohan, T., Donghyun, K., Raghunathan, S., Saraswat, K. "Double-Gate Strained-Ge Heterostructure Tunneling FET (TFET) With record high drive currents and  $\ll 60$  mV/dec subthreshold slope," *Proc. IEEE IEDM*, 1-3 (2008).
- [4] Hoeneisen, B., Mead, C.A., "Fundamental limitations in microelectronics—I. MOS technology," *Solid-State Electronics* 15(7), 819–829 (1972).
- [5] Murphy-Armando, F., Fahy, S., "Giant mobility enhancement in highly strained, direct gap Ge," *J. Appl. Phys.* 109, 113703 (2011)
- [6] Chen, R., Tran, T.-T., Ng, K.W., Ko, W.S., Chang, L.C., Sedgwick, F. G., and Chang-Hasnain, C. "Nanolasers grown on silicon," *Nat. Photonics* 5, 170–175 (2011).
- [7] Tang, M., Chen, S.M, Wu, J., Jiang, Q., Dorogan, V.G., Benamara, M., Mazur, Y.I., Salamo, G.J., Seeds, A., Liu, H., "1.3- $\mu$ m InAs/GaAs quantum-dot lasers monolithically grown on Si substrates using InAlAs/GaAs dislocation filter layers," *Optics Express* 22(10), 11528-11535 (2014).
- [8] Wirth S. et. al., "Optically pumped direct-bandgap GeSn laser", *Nature Photonics* 9, 88–92 (2015)
- [9] Petykiewicz, J., et. al., "Direct Bandgap Light Emission from Strained Germanium Nanowires Coupled with High-Q Nanophotonic Cavities," *Nano Lett.* 16 (4), pp 2168–2173(2016)
- [10] Clavel, M.B. et al., "Heterogeneously-Grown Tunable Tensile Strained Germanium on Silicon for Photonic Devices," *ACS Appl. Mater. Interfaces* 7 (48), pp 26470–26481 (2015)
- [11] Biswas, S., et al, "Non-equilibrium induction of tin in germanium: towards direct bandgap Ge<sub>1-x</sub>Sn<sub>x</sub> nanowires"
- [12] Pavarelli, N., Ochalski, T. J., Murphy-Armando, F., Huo, Y., Schmidt, M. Huyet, G. Harris, J. S., "Optical Emission of a Strained Direct-Band-Gap Ge Quantum Well Embedded Inside InGaAs Alloy Layers," *Phys. Rev. Lett.* 110(17), 177404 (2013)
- [13] Rideau, D., Feraille, M., Ciampolini, L., Minondo, M., Tavernier, C., Jaouen, H., Ghetti, A., "Strained Si, Ge, and Si<sub>1-x</sub>Gex alloys modeled with a first-principles-optimized full-zone k·p method," *Phys. Rev. B* 74, 195208 (2006)
- [14] Tan, S.H., Chang, E.Y., Hudait, M., Maa1, J.S., Liu, C.W., Luo, G.L., Trinh H.D., Su, Y.H., "High quality Ge thin film grown by ultrahigh vacuum chemical vapor deposition on GaAs substrate," *Appl. Phys. Lett.* 98, 161905 (2011)
- [15] Seraphin, B.O., Bottka, N., "Field Effect of the Reflectance in Silicon" *Phys. Rev. Lett.* 15, 104-107 (1965)
- [16] David E. Aspnes, D.E., "Electric Field Effects on the Dielectric Constant of Solids" *Phys. Rev.* 153, 972 (1967)